Available online at www.sciencedirect.com

ScienceDirect

Nuclear Physics B 913 (2016) 381–404

NUCLEAR PHYSICS B

www.elsevier.com/locate/nuclphysb

The physics of antineutrinos in DUNE and determination of octant and δ_{CP}

Newton Nath [a,b,*], Monojit Ghosh [a], Srubabati Goswami [a]

[a] *Physical Research Laboratory, Navrangpura, Ahmedabad 380 009, India*
[b] *Indian Institute of Technology, Gandhinagar, Ahmedabad–382424, India*

Received 23 June 2016; received in revised form 21 September 2016; accepted 22 September 2016

Available online 28 September 2016

Editor: Tommy Ohlsson

Abstract

The octant of the leptonic mixing angle θ_{23} and the CP phase δ_{CP} are the two major unknowns (apart from neutrino mass hierarchy) in neutrino oscillation physics. It is well known that the precise determination of octant and δ_{CP} is interlinked through the octant-δ_{CP} degeneracy. In this paper we study the proficiency of the DUNE experiment to determine these parameters scrutinizing, in particular, the role played by the antineutrinos, the broadband nature of the beam and the matter effect. It is well known that for $P_{\mu e}$ and $P_{\bar{\mu}\bar{e}}$ the octant-δ_{CP} degeneracy occurs at different values of δ_{CP}, combination of neutrino and antineutrino runs help to resolve this. However, in regions where neutrinos do not have octant degeneracy adding antineutrino data is expected to decrease the sensitivity because of the degeneracy and reduced statistics. However we find that in case of DUNE baseline, the antineutrino runs help even in parameter space where the antineutrino probabilities suffer from degeneracies. We explore this point in detail and point out that this happens because of the (i) broad-band nature of the beam so that even if there is degeneracy at a particular energy bin, over the whole spectrum the degeneracy may not be there; (ii) the enhanced matter effect due to the comparatively longer baseline which creates an increased tension between the neutrino and the antineutrino probabilities which raises the overall χ^2 in case of combined runs. This feature is more prominent for IH since the antineutrino probabilities in this case are much higher than the neutrino probabilities due to matter effects. The main role of antineutrinos in enhancing CP sensitivity is their ability to remove the octant-δ_{CP} degeneracy. However even if one assumes octant to be known the addition of antineutrinos can give enhanced CP sensitivity in some parameter regions due to the tension between the neutrino and antineutrino χ^2s.

* Corresponding author at: Physical Research Laboratory, Navrangpura, Ahmedabad 380 009, India.
E-mail addresses: newton@prl.res.in (N. Nath), monojit@prl.res.in (M. Ghosh), sruba@prl.res.in (S. Goswami).

http://dx.doi.org/10.1016/j.nuclphysb.2016.09.017

1. Introduction

The discovery of a non-zero value of the 1–3 leptonic mixing angle θ_{13} by the reactor experiments have established the paradigm of oscillations of the neutrinos amongst three flavours on a firm footing. The parameters involved are: two mass squared differences – Δm^2_{21}, Δm^2_{31}, three mixing angles θ_{12}, θ_{23} and θ_{13} and the CP violating phase δ_{CP}. Among these Δm^2_{21} and θ_{12} are measured by the solar neutrino and the KamLAND reactor neutrino experiments [1]. The information on Δm^2_{31} and θ_{23} has come from Super-Kamiokande (SK) [2] atmospheric neutrino data, as well as from the data of the beam based experiments MINOS [3] and T2K [4]. The best-fit values and 3σ ranges of these parameters are given in [5,6] by analyzing the global neutrino data. The remaining unknown oscillation parameters are (i) the sign of $|\Delta m^2_{31}|$ or the neutrino mass ordering. If we assume the neutrinos to be hierarchical then there can be two types of ordering – the normal hierarchy (NH) corresponding to $m_1 \ll m_2 \ll m_3$ and $\Delta m^2_{31} > 0$ and the inverted hierarchy (IH) corresponding to $m_2 \approx m_1 \gg m_3$ and $\Delta m^2_{31} < 0$, (ii) the octant of θ_{23} – with $\theta_{23} < 45°$ corresponding to lower octant (LO) and $\theta_{23} > 45°$ corresponding to higher octant (HO) and (iii) the CP violating phase δ_{CP} for which the full range from $-180° < \delta_{CP} < 180°$ is still allowed at 3σ C.L. [5,6]. Information on these parameters can come from the currently running superbeam experiments T2K [7] and NOνA [8,9]. However this is possible only for favourable values of parameters. The main problem which these experiments can face is due to parameter degeneracies by which it is meant that different parameters giving equally good fit to the data. With θ_{13} unknown, an eight-fold degeneracy was identified which would make the precise determination of parameters difficult [10]. These were intrinsic θ_{13} degeneracy [11], hierarchy-δ_{CP} degeneracy [12] and octant degeneracy [13]. With the precise determination of θ_{13} [14–17] and inclusion of spectral information the intrinsic degeneracy is now solved. However the lack of knowledge of hierarchy, octant and δ_{CP} can still give rise to degenerate solutions which can affect the sensitivities of these experiments towards these parameters [18–22].

In this paper our focus is on the determination of the octant of θ_{23} and the CP phase δ_{CP}. Currently the most precise measurements of the parameter θ_{23} comes from the T2K experiment. The primary channel for this is the survival probability $P_{\mu\mu}$. For baselines shorter than 1000 km this probability is a function of $\sin^2 2\theta_{23}$ to the leading order and suffers from an intrinsic octant degeneracy which refers to the same value of probability for θ_{23} and $\pi/2 - \theta_{23}$. The leading order term of the appearance channel probability $P_{\mu e}$ depends on the combination $\sin^2\theta_{23} \sin^2 2\theta_{13}$. Although this does not exhibit intrinsic octant degeneracy, there can be uncertainties due to the $\sin^2\theta_{13}$ factor. It was shown in [23,24] that combining the reactor measurement of θ_{13} with the accelerator data will be helpful for extraction of information on octant from this channel. Thus, the precise measurement of θ_{13} from the reactor experiments is expected to enhance the octant sensitivity coming from this channel. The combination of the disappearance and appearance channel measurements in long baseline experiments can also be helpful in resolving octant degeneracy because of the different functional dependence of the two probabilities on θ_{23}. This creates a synergistic effect so that the octant sensitivity of both channels combined is higher [19,21,25]. T2K collaboration has performed a full three flavour analysis using information from both $(\nu_\mu - \nu_\mu)$ and $(\nu_\mu - \nu_e)$ channels. They obtain best-fit $\sin^2\theta_{23} \sim 0.52$ with a preference for NH [7]. MINOS collaboration has also completed their combined analysis of disappearance and appearance data and have also included atmospheric neutrino data in their analysis [3]. They get a best-fit at $\sin^2\theta_{23} = 0.41$ for IH. The first NOνA disappearance results with 2.74×10^{20} protons on target, give best-fit of $\sin^2\theta_{23} = 0.43 \oplus 0.60$ [9]. The latest analysis of Super Kamiokande atmospheric neutrino data shows a weak preference for NH-HO [26]. Global analysis of neutrino data including all the different information gives the best-fit in LO for NH and in HO for IH [5,6]. Thus it is clear from the above discussion that at present the situation regarding octant of θ_{23} is quite intriguing.

There have been studies on the possibility of determining the octant from combined study of the experiments T2K and NOνA using their full projected exposure [19,25]. It was observed that the main problem in octant resolution arises due to the unknown value of δ_{CP} in the subleading terms of $P_{\mu e}$ which gives rise to octant–δ_{CP} degeneracy. Also, the lack of knowledge about hierarchy can create further problem with the occurrence of wrong hierarchy–wrong octant solutions [22]. Recently it was pointed out in [19,21] that equal neutrino and antineutrino runs can help in resolving octant–δ_{CP} degeneracy. The reason being the octant–δ_{CP} combination suffering from degeneracy in neutrino probabilities are not degenerate for the antineutrino probabilities. It was shown for instance in [19] that combining T2K and NOνA running in equal neutrino and antineutrino mode for 2.5 years each and 3 years each respectively can identify the correct octant at 2σ C.L. irrespective of hierarchy and δ_{CP} if $\theta_{23} \leq 41°$ or $\geq 49.5°$.

The degeneracies can also be alleviated if neutrinos pass through large distances in matter so that resonant matter effects develop. This is the case of the atmospheric neutrinos passing through matter. In this case the leading order term in $P_{\mu e}$ goes as $\sin^2\theta_{23}\sin^2 2\theta_{13}^m$. However, since at resonance $\sin^2 2\theta_{13}^m \approx 1$, the octant degeneracy is resolved. Further, the $P_{\mu\mu}$ channel also contains an octant sensitive term $\sin^4\theta_{23}\sin^2 2\theta_{13}^m$ which enhances the sensitivity [27]. Octant sensitivity can also come from the Δm^2_{21} dependent term which gives rise to an excess of sub-GeV electron like events for the atmospheric neutrinos [28,29]. In addition the antineutrino component in atmospheric neutrino flux can also help in resolving octant ambiguity. It was shown that combined analysis of T2K and NOνA with atmospheric neutrino data can give enhanced octant sensitivity [25]. The effect was found to be larger in multi-megaton water detectors like PINGU [30] or a LArTPC detector, sensitive to both muon and electron events [25].

The current best-fit value for δ_{CP} is close to $-\pi/2$ although at 3σ C.L. the whole range of $[0, 2\pi]$ remains allowed [5,6]. The δ_{CP} sensitivity of an experiment is often understood in terms of the CP asymmetry between the neutrinos and antineutrinos.

$$A_{cp} = \frac{P_{\mu e} - P_{\bar{\mu}\bar{e}}}{P_{\mu e} + P_{\bar{\mu}\bar{e}}} \sim \frac{\sin\delta_{CP}}{\sin\theta_{13}} \tag{1}$$

However the diagnostics used for probing CP violation is the sum total of the χ^2 contribution of the neutrinos and antineutrinos: $\chi^2_{total} = \chi^2_\nu + \chi^2_{\bar{\nu}}$ which does not show the above dependence [31]. Hence one needs to understand the actual role played by antineutrinos, if any, for determination of CP violation. Indeed one already has a hint for non-zero δ_{CP} from only neutrino runs of T2K and NOνA. Whereas the confirmation of CP violation independently from antineutrino runs in these experiments cannot be undermined, it has already been observed in the case of T2K that unless the parameter space contains octant degeneracy the antineutrinos do not play any role for discovery of CP violation [32,33]. However for the NOνA experiments antineutrinos seem to be playing some role even when there is no octant degeneracy [32]. In this work, it is one of our goals to understand the role of antineutrinos for enhancing CP sensitivity for the DUNE baseline. In particular we explore whether the antineutrino runs can play any non-trivial contribution to the total χ^2 if octant and hierarchy are assumed to be known and if so then what are the physics issues involved.

The current generation superbeam experiments T2K and NOνA are off-axis experiments using narrow band beams to reduce the backgrounds at the high energy tail. However the future generation high statistics accelerator experiments plan to use on-axis configurations and high intensity wide band beams enabling them to explore oscillations over a larger energy range. The examples for this are the European initiative LBNO and LBNE which was proposed in US using the FermiLab beamline. In 2014 it was proposed to combine these activities in a coherent international long-baseline neutrino program hosted at Fermilab with the detector at the Sanford Underground Research Facility (SURF) in South Dakota. On Jan. 30, 2015 the LBNE collaboration was officially dissolved, the new collaboration selected the name Deep Underground Neutrino Experiment (DUNE). The baseline is 1300 km and the proposed detector is a 40 kt (or 34 kt) modular Liquid Argon Time Projection Chamber (LArTPC) with the first phase being a 10 kt detector. There are several studies of the physics prospects of a 1300 km baseline LArTPC using a wide band beam [34]. In particular octant and/or CP sensitivity of such a set-up has been considered in [35–40]. In [35] the octant and CP sensitivity reach of a 10 kt LArTPC detector for LBNE combined with T2K and NOνA was studied. In [36] the minimum exposure for DUNE in conjunction with T2K, NOνA and ICAL@INO experiment was computed for giving a octant sensitivity with $\Delta\chi^2 = 25$ and a CP sensitivity with $\Delta\chi^2 = 9$ for 40% and ∼70% coverage of δ_{CP}. In [37] the octant sensitivity of a 10 kt and 35 kt detector was studied with and without the near detector and also the role of precise knowledge of θ_{13} coming from reactor experiments, in improving the sensitivities were studied. In [38] octant and CP sensitivity results were presented for a 10 kt detector and effect of including a near detector as well as the role of atmospheric neutrinos were considered. In [39] octant and CP sensitivity of a 35 kt detector, with and without magnetization, was studied. All these papers considered equal neutrino and antineutrino run for the octant sensitivity. Variation of proportion of neutrino and antineutrino run was studied in [36] for only IH and $\theta_{23} = 39°$ for octant sensitivity and NH and $\theta_{23} = 51°$ for CP sensitivity. This issue was also discussed in [41] for a setup with a baseline of 1540 km where they concluded that for true hierarchy as NH equal neutrino and antineutrino run is better whereas for true hierarchy as IH 30% antineutrino run is optimal. These conclusions were drawn for true $\theta_{23} = 45°$ and the results were presented in terms of fraction of δ_{CP} for which a 3σ signal of CP violation can be obtained.

In this work, our main goal to understand the role of antineutrinos for enhancing octant and CP sensitivity for the DUNE baseline. In particular, we study the impact of the broadband nature of the beam and the role of enhanced matter effects as compared to the currently running beam-based experiments T2K and NOνA which have shorter baselines and hence less matter effects. To the best of our knowledge these features have not been emphasized earlier in the literature. In particular, a deeper understanding of the role played by antineutrinos will help in optimizing the amount of antineutrino run. We present the results of the octant sensitivity using different combinations of neutrino–antineutrino run (i) as a function of true δ_{CP} for fixed values of true θ_{23} (ii) as a function of true θ_{23} for fixed values of true δ_{CP} and (iii) also in the true (θ_{23}–δ_{CP}) plane. These three kinds of plots allow us to study the dependence of octant-sensitivity on these two parameters in an exhaustive manner. In addition we present the allowed regions in the true-θ_{23}–test θ_{23} plane for both hierarchies and for true $\delta_{CP} = \pm 90°$. These plots give the precision of θ_{23} at these values of δ_{CP}. It is worthwhile to mention here that one of the main aims of the DUNE collaboration is to measure the parameter δ_{CP} which underscores the importance of combining neutrino and antineutrino runs. However the main role that the antineutrinos play in

Table I
Representative values of neutrino oscillation parameters.

	$\sin^2 2\theta_{13}$	$\sin^2\theta_{12}$	θ_{23}	$\Delta m^2_{21}(\mathrm{eV}^2)$	$\Delta m^2_{31}(\mathrm{eV}^2)$	δ_{CP}
True values	0.1	0.31	35°–55°	7.60×10^{-5}	2.40×10^{-3}	−180° to +180°
Test values	0.085–0.115	Fixed	35°–55°	Fixed	$(2.15–2.65)\times10^{-3}$	−180° to +180°

the determination of δ_{CP} is the removal of octant degeneracy and thus both issues are intimately connected. To emphasize this point we also present the figures showing the CP discovery potential of DUNE for the cases when octant is assumed to be known and unknown. In particular we explore whether the antineutrino runs can play any non-trivial contribution to the total χ^2 if octant and hierarchy are assumed to be known and if so then what are the physics issues involved. We study how much fraction of antineutrino run is optimum for values of θ_{23} in lower and upper octants and in addition to the CP fractions, also show explicitly which are the CP values for which antineutrino run can be important. Note that most of the earlier works in literature have considered equal neutrino and antineutrino run for determination of octant and δ_{CP} in DUNE. We present the results by varying the antineutrino component in the run. This constitutes another new feature of our study.

The plan of the paper goes as follows: in the next section we give the experimental and simulation details of DUNE that have been taken into consideration. In Section 3 we discuss the physics of the octant and CP sensitivity of the DUNE experiment in detail. In Section 4 we present our results. Section 4.1 contains the results for octant sensitivity and Section 4.2 is devoted for the discussions on CP sensitivity and role of antineutrinos in DUNE. Finally we summarize and conclude in Section 5.

2. Experimental and simulation details

In this paper we have simulated the DUNE experiment using the GLoBES package [42,43]. In our simulation, we have considered a 10 kt configuration of the detector. This experiment is based on the existing Neutrinos at the Main Injector (NuMI) beamline design and the beam flux peaks at 2.5 GeV. Far detector will be located 4,850 feet underground. One of the options for DUNE is to have an initial beam power of 1.2 MW which will be increased to 2.3 MW later [44]. In our simulation we consider neutrino flux [45] corresponding to 1.2 MW beam power which gives 10^{21} protons on target (POT) per year. This corresponds to a proton energy of 120 GeV. In Table I we list the representative values for the neutrino oscillation parameters that we have used in our numerical simulation. These values are consistent with the results obtained from global-fit of world neutrino data [46–48]. Systematic errors are taken into account using the method of pulls [49,50] as outlined in [51]. We have also added 5% prior on $\sin^2 2\theta_{13}$ in our numerical simulation. The systematic errors and efficiencies corresponding to signal and background are taken from [34]. Note that the values of these quantities given in [44] are somewhat different. Using these may change our numerical results to some extent though the main physics issues addressed in this work will not be altered.

3. Physics of octant sensitivity for a 1300 km baseline

The probabilities that are relevant for the DUNE experiment are $P_{\mu e}$ and $P_{\mu\mu}$ and the corresponding probabilities for the antineutrinos. In presence of matter, the relevant oscillation probabilities can be expanded perturbatively in terms of small parameters $\alpha(\equiv \Delta m^2_{21}/\Delta m^2_{31})$ and θ_{13} as follows, [52–54]

$$P_{\mu e} = \underbrace{4 s^2_{13} s^2_{23} \frac{\sin^2(A-1)\Delta}{(A-1)^2}}_{\mathcal{O}_o} + \underbrace{\alpha^2 \cos^2\theta_{23} \sin^2 2\theta_{12} \frac{\sin^2 A\Delta}{A^2}}_{\mathcal{O}_2} \tag{2}$$

$$\underbrace{+\,\alpha s_{13} \sin 2\theta_{12} \sin 2\theta_{23} \cos(\Delta + \delta_{cp}) \frac{\sin(A-1)\Delta}{(A-1)} \frac{\sin A\Delta}{A}}_{\mathcal{O}_1}$$

$$P_{\mu\mu} = 1 - \sin^2 2\theta_{23} \sin^2\Delta + \mathcal{O}(\alpha, s_{13}) \tag{3}$$

where,

$$\Delta \equiv \frac{\Delta m^2_{31} L}{4E},\ A \equiv \frac{2EV}{\Delta m^2_{31}} \equiv \frac{VL}{2\Delta},\ \text{and } V = \pm\sqrt{2} G_F n_e \tag{4}$$

These expressions are derived assuming constant matter density approximation. Similar expressions for antineutrino probabilities can be obtained by replacing $\delta_{CP} \to -\delta_{CP}$ and $V \to -V$. The '$+(-)$' sign here represents neutrino (antineutrino). For NH, Δm^2_{31} is positive and for IH, Δm^2_{31} is negative. Hence, in the neutrino oscillation probability A is positive for NH and negative for IH. For antineutrinos, the sign of A gets reversed.

It is clear from the above expressions that to leading order $P_{\mu\mu}$ suffers from intrinsic octant degeneracy between θ_{23} and $\pi/2 - \theta_{23}$. $P_{\mu e}$ does not suffer from intrinsic degeneracy and the octant sensitivity comes mainly from this channel. However since $P_{\mu e}$ depends on $\sin^2\theta_{23}$, the χ^2 is an increasing function of θ_{23} for this case and the wrong octant minima from this channel always occurs for 45°. On the other hand $P_{\mu\mu}$ forces the minima to $\sim \pi/2 - \theta_{23}$, where the appearance channel has a large octant sensitive contribution.

However although $P_{\mu e}$ does not suffer from intrinsic degeneracy it is possible to have

$$P_{\mu e}(\Delta, \theta^{tr}_{23}, \delta^{tr}_{CP}) = P_{\mu e}(\Delta, \theta^{wr}_{23}, \delta^{wr}_{CP}), \tag{5}$$

where the suffix tr (wr) denotes the true (wrong) values of the parameters. The above equation implies that apart from the true solution one can also get duplicate solutions with right hierarchy–wrong octant–wrong δ_{CP} (RH–WO–Wδ_{CP}). Note that unlike in the case of $P_{\mu\mu}$, for $P_{\mu e}$ one needs to consider the variation of θ_{23} over the whole of the opposite octant in order to identify the degenerate solution. Apart from this, if the hierarchy is unknown then one can also have

$$P_{\mu e}(\Delta, \theta^{tr}_{23}, \delta^{tr}_{CP}) = P_{\mu e}(-\Delta, \theta^{wr}_{23}, \delta^{wr}_{CP}). \tag{6}$$

This corresponds to solutions with wrong hierarchy–wrong octant–wrong δ_{CP} (WH–WO–Wδ_{CP}). As pointed out in [22] the most generalized case assuming θ_{13} as fixed, gives rise to total eight possibilities corresponding to different combinations of right (wrong) hierarchy and/or octant and/or δ_{CP}. From Fig. 1 one can see that for the DUNE baseline degenerate solutions with right-δ_{CP} do not come unlike the case of the experiments T2K and NOνA [22]. This is because due to matter effects the bands for NH and IH are much more well separated and hence the intersection at right δ_{CP} do not occur. In this work we show how the octant sensitivity is affected by the wrong solutions defined in Eqs. (5) and (6). We also discuss how the δ_{CP} sensitivity is affected by the occurrence of wrong octant solutions. We put emphasis on the role of antineutrinos and point out some unexpected behaviour due to matter effects.

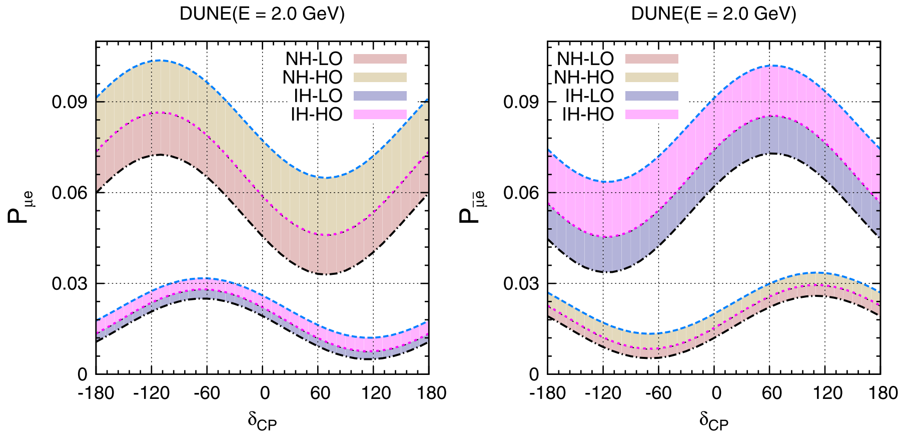

Fig. 1. Left panel (right panel) represents $P_{\mu e}$ ($P_{\bar{\mu}\bar{e}}$) for DUNE. Here the bands are over current 3σ range of θ_{23} [48]. For LO, NH (LO, IH) we consider the range of θ_{23} over 38.8°–45° (39.4°–55°) and for HO, NH (HO, NH) we consider the range of θ_{23} over 45°–53.3°(45°–53.1°).

Fig. 1 describes the oscillation probability in presence of earth matter for $L = 1300$ km and $E = 2$ GeV. The bands are due to the variation of θ_{23} (see figure caption for details). The neutrino oscillation probability for NH gets significant enhancement in presence of earth's matter as compared to IH as shown in the left panel. It is seen that the maximum probability for NH can become more than 3-times than that of IH. But in the case of antineutrinos the scenario gets reversed as A and δ_{CP} changes their sign, as can be observed in the right panel. This can be understood from Eq. (2) that the $\mathcal{O}_o$ term is Δ dependent which enhances the probability value for the given set of oscillation parameters for NH as compared to IH for neutrino and ($\mathcal{O}_1, \mathcal{O}_2$) terms are α and α^2 suppressed respectively.

Note that for vacuum oscillation maxima, Δ corresponds to 90°. Thus in the appearance channel probability (cf. Eq. (2)), $\delta_{CP} = -90°(+90°)$ correspond to maximum (minimum) point in the probability for neutrinos. For antineutrinos it is the opposite. Thus, for these values of δ_{CP}, octant sensitivity is expected to be maximum if there is no degeneracy. Note that with the inclusion of matter effect, the appearance channel probability maxima does not coincide with the vacuum maxima and in that case the maximum and minimum points in the probability do not come exactly at $\pm 90°$ but gets slightly shifted. This can be seen from Fig. 1. However for illustration, we will take $\delta_{CP} = \pm 90°$ as the reference points to describe the physics of octant in DUNE.

It is to be observed that, if we draw a horizontal line at particular probability value then the different intersection points with the given band lead to different degenerate solutions. The occurrence of octant degeneracies that can be inferred from these plots are summarized in Table II. From the above discussions as well as from earlier studies it is clear that the nature of octant–δ_{CP} degeneracy is different for neutrinos and antineutrinos and therefore combined neutrino–antineutrino run is helpful for resolving the octant degeneracy [19,21,35]. Also note that the behaviour of octant–δ_{CP} degeneracy in neutrinos and antineutrinos is same for both NH and IH.

The probability plot as given in Fig. 1 is done for an energy of 2 GeV. However it is possible that because of the broad-band nature of the beam the occurrence of degeneracy at a particular energy may not be true over the whole energy range. Thus for DUNE, one can still get some

Table II
The octant degenerate parameter space for neutrinos and antineutrinos. Here, LO = Lower octant, HO = Higher octant, UHP = Upper half plane ($0^\circ < \delta_{CP} < 180^\circ$) and LHP = Lower half plane ($-180^\circ < \delta_{CP} < 0^\circ$).

Octant degeneracy	ν	$\bar{\nu}$
LHP, LO	degenerate with UHP, HO	no degeneracy
UHP, LO	no degeneracy	degenerate with LHP, HO
LHP, HO	no degeneracy	degenerate with UHP, LO
UHP, HO	degenerate with LHP,LO	no degeneracy

amount of octant sensitivity, even in the degenerate parameter space outlined in Table II, when integrated over all the energy bins.

It is to be noted that Fig. 1 does not demonstrate any hierarchy degeneracy since the two bands corresponding to NH and IH remain non-overlapping. However conclusions drawn at probability level need to be substantiated by a proper χ^2 analysis to determine with what significance the hierarchy degeneracy is actually resolved by DUNE. Therefore we will present the results of octant sensitivity either for both cases – right and wrong hierarchy or by marginalizing over the hierarchy.

4. Results

4.1. Octant discovery χ^2 for a 10 kt detector

In this section we discuss the octant sensitivity of DUNE for a 10 kt detector volume which is the projected detector volume for DUNE in the first phase. The statistical χ^2 for octant sensitivity is calculated by taking the correct octant in the true spectrum and the wrong octant in the test spectrum in the following formula

$$\chi^2_{\rm stat} = \sum_i 2\left[N_i^{\rm test} - N_i^{\rm true} - N_i^{\rm true}\log\left(\frac{N_i^{\rm test}}{N_i^{\rm true}}\right)\right], \tag{7}$$

where N_i is the number of events in the ith energy bin. In Fig. 2 we show the χ^2 for octant discovery which is the combined sensitivity coming from appearance channel, disappearance channel and $\sin^2 2\theta_{13}$ prior i.e.,

$$\chi^2 = \chi^2_{ap} + \chi^2_{disap} + \chi^2_{prior} \tag{8}$$

as a function of true δ_{CP}.

We consider the representative true values of $\theta_{23} = 39^\circ$ for LO and $\theta_{23} = 51^\circ$ for HO. χ^2 is marginalized over test values of θ_{23} over opposite octant. We give the plots separately for true and false hierarchy. This shows for what parameters and to what extent the octant sensitivity is affected by the lack of knowledge of hierarchy. Depending on the true parameters, we get four combinations of (hierarchy–octant): NH-LO, NH-HO, IH-LO, IH-HO. For all the plots in the upper row of Fig. 2, dark-blue curves are for True(NH)–Test(NH) and magenta curves are for True(NH)–Test(IH) while for the lower row dark-blue curves correspond to True(IH)–Test(IH) and magenta curves correspond to True(IH)–Test(NH). Below we discuss the results for each true combination.

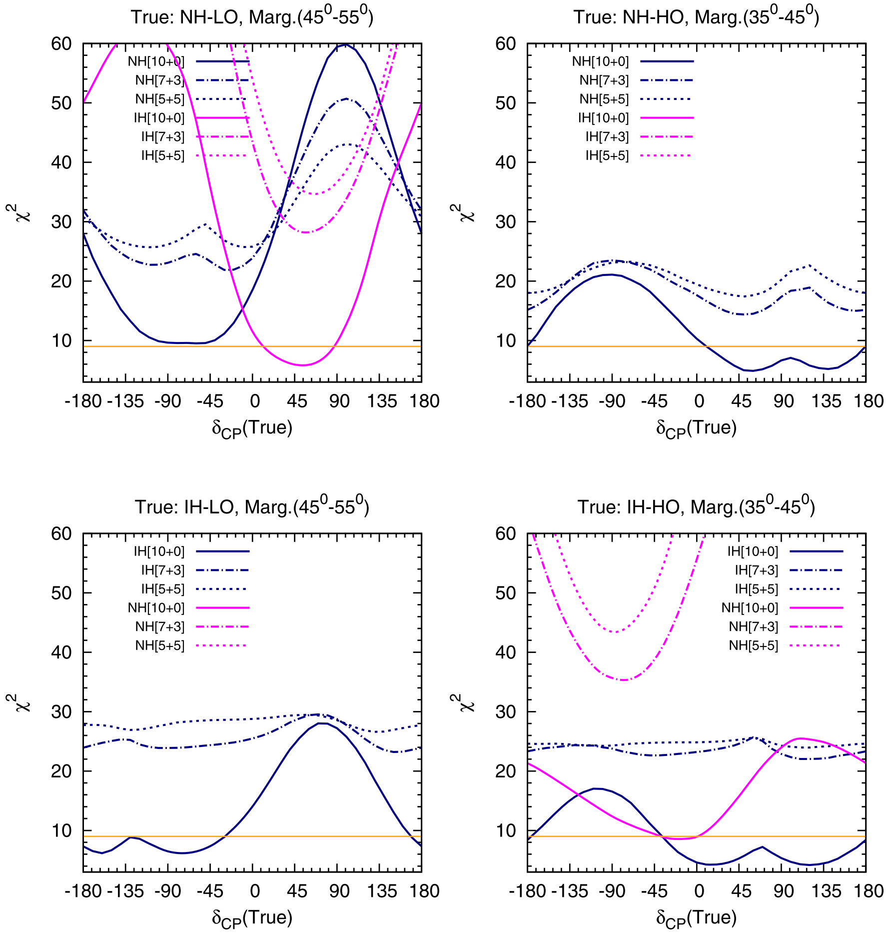

Fig. 2. Octant discovery χ^2 for DUNE. Left (right) panel is for LO (HO), where true(θ_{23}) is considered as 39° (51°) and test(θ_{23}) is marginalized over (45° to 55°) for LO and (35° to 45°) for HO. The labels NH, IH inside the plots signify test hierarchy.

- **NH-LO** ($\theta_{23}^{\text{true}} = 39°$): The figure for true NH-LO shows that for values of δ_{CP} in the lower half plane, a 10 year neutrino run of DUNE can resolve the octant degeneracy at 3σ C.L. The inclusion of antineutrino run helps in enhancing the octant sensitivity for δ_{CP} in LHP ($-180° < \delta_{CP} < 0°$) and θ_{23} in LO since the antineutrino probability is devoid of octant degeneracy. Note that in this case though pure neutrino run suffers from octant degeneracy, still we get χ^2 around 10. This is one of the unique features of the broad-band beam where the degeneracy does not exist over the entire energy range and one can still have some octant sensitivity from the neutrino channel. For the UHP ($0° < \delta_{CP} < 180°$) on the other hand the neutrino data gives a better octant sensitivity since antineutrinos are plagued with degeneracies for LO, as shown by the blue curves. However the scenario changes if we assume the hierarchy is not known. In that case the antineutrino run is seen to help to remove wrong hierarchy–wrong octant solutions in-spite of having degeneracies, as is seen from the magenta curves. In order to understand this point we have plotted the appearance channel

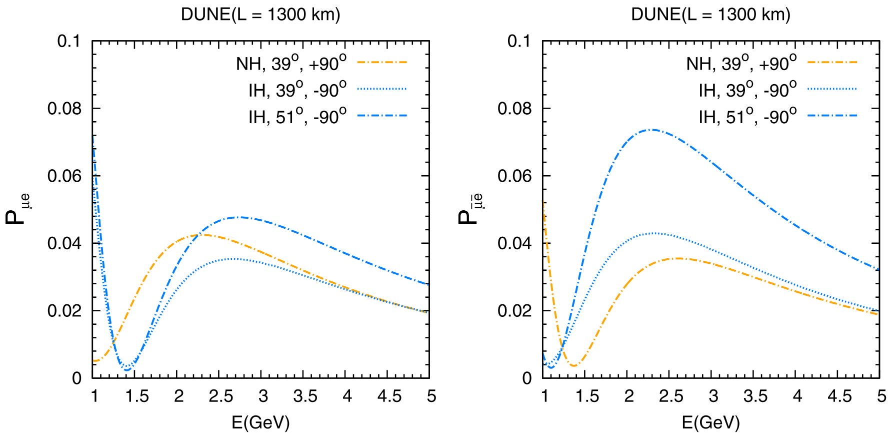

Fig. 3. Here, left panel (right panel) represents $P_{\mu e}$ ($P_{\overline{\mu}\overline{e}}$) as a function of energy for DUNE and hierarchy corresponds to orange (light blue) curve is NH (IH). (For interpretation of the references to color in this figure, the reader is referred to the web version of this article.)

probability vs energy in Fig. 3. The left panel is for neutrinos and the right panel is for antineutrinos. In the left panel we see that the orange curve ($\delta_{CP} = +90°$) is well separated from the dotted blue curve ($\delta_{CP} = -90°$) near the oscillation maxima for $\theta_{23} = 39°$. But when marginalized over θ_{23}, the dashed blue curve which corresponds to $\delta_{CP} = -90°$ and $\theta_{23} = 51°$, overlaps with the orange curve to give WH–WO–Wδ_{CP} solution.[1] On the other hand in the right panel we see that due the marginalization of θ_{23} the dashed blue curve moves far away from the orange curve resolving the degeneracy. Note that if we marginalize over hierarchy then for UHP the minimum will come at the WH solution with only neutrino data and hence octant degeneracy is not resolved at 3σ for $9° < \delta_{CP} < 90°$ belonging to the UHP. However with $7 + 3$ years run the octant degeneracy is resolved with a $\chi^2 > 25$ even without the knowledge of the true hierarchy for all values of δ_{CP}. With $5 + 5$ year run in most part of UHP the minima occurs with the RH solution. But for $45° < \delta_{CP} < 115°$, the WH minima is below the one with RH.

- **NH-HO** ($\theta_{23} = 51°$) For this case from Fig. 1 it is seen that for ($51°, -90°$, NH) no octant degeneracy prevails at the probability level for neutrinos whereas antineutrinos have octant degeneracy. Also, antineutrinos have less statistics. Thus we expect that only neutrino run should give a better sensitivity. But, we notice from the top right figure of Fig. 2, that addition of antineutrino gives higher χ^2 value as compared to only neutrino mode [$10 + 0$]. In order to understand this feature in the first panel of Fig. 4 we plot the χ^2 vs test δ_{CP}.
  The curve for only antineutrinos indeed confirm the occurrence of degeneracies close to $\delta_{CP} \sim 90°$. However at that point the neutrino χ^2 is very high. Thus, when the neutrino and antineutrino data are combined the overall minima is governed by the neutrinos and so comes close to the true value of $\delta_{CP} = -90°$. At this point both neutrinos and antineutrinos have octant sensitive contribution. This is shown in Table III where we illustrate the contributions from the neutrinos and antineutrinos separately for the appearance channel. It is evident that as we increase the antineutrino component the contribution from neutrino channel reduces

[1] Due to the presence of $P_{\mu\mu}$ channel, the wrong octant minima comes around $\theta_{23} = 51°$ for true $\theta_{23} = 39°$.

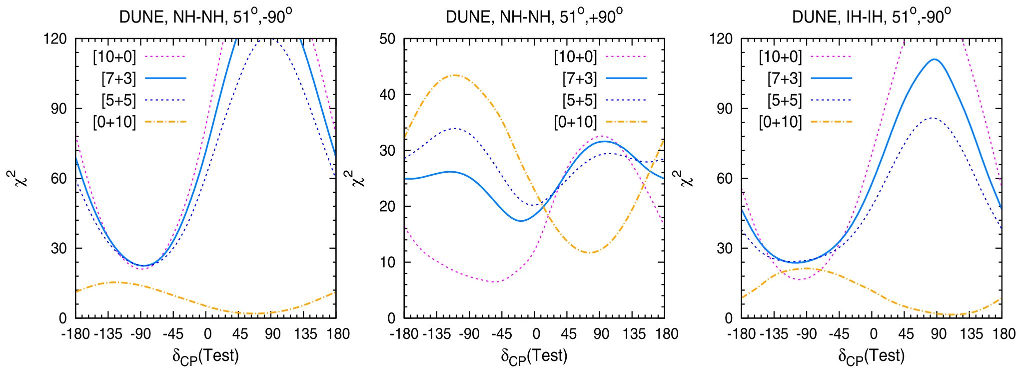

Fig. 4. Octant χ^2 vs test (δ_{CP}) for DUNE.

Table III
Here, $[10+0]$, $[7+3]$ and $[5+5]$ refers to $(\nu+\bar{\nu})$ runs of DUNE, where as $(8+0)$, $(5+3)$ and $(4+4)$ refers to $(\nu+\bar{\nu})$ runs of T2K. The numbers in the parenthesis correspond to T2K. Also "Test parameters" refer to the test values where χ^2 minimum appears and remaining oscillation parameters are same as true parameters.

$(\nu+\bar{\nu})$	Test parameters	$\chi^2_{ap,\nu}$	$\chi^2_{ap,\bar{\nu}}$	$\chi^2_{disap,(\nu+\bar{\nu})}$	Prior	Total
	NH, 51°, −90°(true)					
$[10+0](8+0)$	$\theta_{23}=41.5°(41°)$	11.5(6.65)	0	0.5(0.35)	9(1.44)	21.05(8.44)
	$\sin^2 2\theta_{13}=0.115(0.106)$					
$[7+3](5+3)$	same as $[10+0](8+0)$	9.14(4.28)	1.99(1.44)	1.97(0.37)	9(1.44)	22.46(7.18)
$[5+5](4+4)$	same as $[10+0](8+0)$	7.21(3.46)	2.98(1.44)	3.34(0.37)	9(1.44)	22.52(6.72)
	IH, 51°, −90°(true)					
$[10+0](8+0)$	$\theta_{23}=40°$ (41°),	10.86(5.23)	0	0.09(1.47)	5.76(1.44)	16.71(8.14)
	$\delta_{CP}=-105°(-90°)$					
	$\sin^2 2\theta_{13}=0.112(0.106)$					
$[7+3](5+3)$	same as $[10+0](8+0)$	8.22(3.36)	8.10(1.33)	1.62(0.96)	5.76(1.44)	23.71(7.09)
$[5+5](4+4)$	$\theta_{23}=40.5°(41°)$,	6.46(3.37)	9.78(2.08)	2.14(0.84)	5.76(0.36)	24.15(6.66)
	$\delta_{CP}=-120°(-90°)$					
	$\sin^2 2\theta_{13}=0.112(0.103)$					

whereas that from the antineutrino channel increases. Thus although the antineutrino channel has degeneracy the minima does not come at the point of degeneracy as it is governed by the neutrinos. Even then the total $\chi^2(=\chi^2_{ap,\nu}+\chi^2_{ap,\bar{\nu}})$ from appearance channel (11.13, 10.19), corresponding to $[7+3]$ and $[5+5]$ respectively, is less than the pure neutrino run. However, the total χ^2 for the mixed run is higher.

To understand this point we list the contribution from the disappearance χ^2 and it is seen that although for pure neutrino run the disappearance channel does not have any octant sensitive contribution to the total χ^2 for mixed runs this channel also provide some octant sensitivity. This arises because due to matter effects the neutrino and antineutrino probabilities are different and hence the χ^2 minima comes at different places. When one combines neutrino and antineutrino run then this creates a synergy and hence some octant sensitivity arises from the disappearance channel also. Due to this reason when one combines appearance and disappearance channels then addition of antineutrino runs actually gives a slight increase in χ^2. In the UHP on the other hand the octant sensitivity increases with antineutrino run. This is clear since for $P_{\mu e}$ the neutrino channel suffers from octant degeneracy whereas the antineutrino channel does not and the addition of antineutrinos help to overcome the degeneracy. To illustrate this point further in the middle panel of Fig. 4 we plot the χ^2 vs test δ_{CP} for true values (51°, 90°). In this case the pure neutrino run gives the minima in the LHP close to $\delta_{CP} \sim -45°$ whereas pure antineutrino gives minima near the true value. However when we combine neutrino and antineutrino runs then the overall minima comes in between and moves towards the antineutrino minima as the $\bar{\nu}$ component is increased. At this point there is octant sensitive contribution from both neutrinos and antineutrinos. Thus the antineutrino data helps in this case by trying to shift the minima away from the degenerate point. We also compare the χ^2 for DUNE with that of T2K, given in parentheses in Table III, to understand the role of broadband beam and enhanced matter effect. It is seen from the last column that for T2K the χ^2 reduces with increasing antineutrinos as is expected. Note that this is in contrast to DUNE due to its broadband nature and enhanced matter effect.

- **IH-LO** ($\theta_{23} = 39°$): In this case for LHP the antineutrino run enhances the sensitivity because they do not suffer from octant degeneracy as can be seen from Table II. But for the UHP the antineutrino probability has octant degeneracy. Thus again we expect that in UHP adding antineutrino data should reduce the sensitivity. But the figure shows a slight enhancement. This can again be explained by similar reasoning as for the NH, 51° and −90° case. There is also the finite contribution from the disappearance channel enhancing the octant sensitivity when the neutrino and antineutrino runs are combined. These combinations of hierarchy−octant can resolve octant degeneracy at 5σ C.L. with $[5 + 5]$ years of $[\nu + \bar{\nu}]$ run for any value of true δ_{CP} as shown in Fig. 2.
- **IH-HO** ($\theta_{23} = 51°$): For this case, for δ_{CP} in LHP the octant sensitivity with pure neutrino run is seen to be above $\chi^2 = 9$ in the interval $-180° < \delta_{CP} < -45°$. Adding antineutrino data helps to raise the χ^2 for octant sensitivity. As before we ask the question how antineutrino data is helpful despite the presence of degeneracies in this channel. This can be explained again similar to the NH-HO case. The third panel of Fig. 4 shows that for pure antineutrinos, there is very small octant sensitivity and the minima comes in the UHP between 90° and 135°. However at the point, in the LHP, where the pure neutrino χ^2 is minimum, antineutrino χ^2 has a large non-zero value and for combined runs the minima is still governed by the neutrinos. Thus the contributions from the antineutrinos are also being added up in-spite of having degeneracy. The neutrino and antineutrino contributions from the appearance channel are shown in Table III. It is seen that for IH, because of the enhancement of the antineutrino probability due to matter effect, a large octant sensitive contribution to the χ^2 is obtained. The disappearance channel also gives a small contribution but the contribution from the antineutrino channel is almost comparable or larger than the neutrino channel. It is also to be noted that if hierarchy is not known then for some values of δ_{CP} the minima comes in the wrong hierarchy region for pure neutrino run and the sensitivity is further reduced. Addition of antineutrinos resolves the hierarchy with $\chi^2 \geq 25$ and so the minima does not occur anymore for wrong hierarchy solution. For the UHP the only neutrino run has very poor sensitivity due to degeneracies with δ_{CP} and addition of antineutrino runs help. The UHP is more favourable for resolution of hierarchy–δ_{CP} degeneracy and even with only neutrino run hierarchy is resolved at 3σ for all values of δ_{CP}. Overall, close to $\chi^2 = 25$ sensitivity is achieved for this combination of hierarchy and θ_{23} with $7 + 3$ or $5 + 5$ combination for the whole range of δ_{CP}. For this case also in Table III the T2K χ^2 values are given in parentheses. It is seen from the last column that the overall χ^2 for T2K decreases with enhanced antineutrinos unlike that in DUNE. If one compares the appearance χ^2 values for the

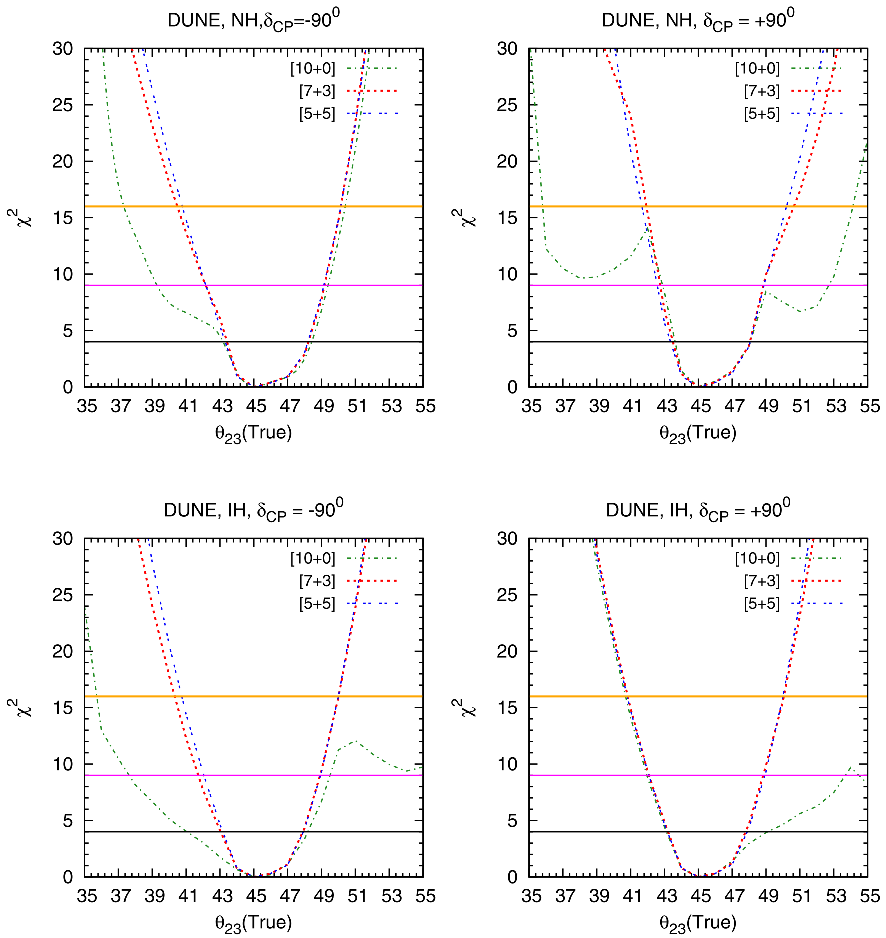

Fig. 5. Octant sensitivity χ^2 for DUNE. Left (right) panel is for $\delta_{CP} = -90°$ ($+90°$), where true hierarchy is considered as NH (IH) for upper (lower) row. Here black, magenta and yellow lines represent χ^2 value at 2σ, 3σ and 4σ respectively.

antineutrino channel for DUNE and T2K then it is seen that the contribution of this channel for DUNE is quite high and comparable or even greater than the neutrino contribution. This is due to the enhanced matter effect associated with IH and HO for the longer baseline of DUNE.

After discussing the role of antineutrinos and disappearance channel in octant sensitivity for DUNE, in Fig. 5 we present the octant χ^2 as a function of true θ_{23} for maximal CP violation. Depending on if the true hierarchy is NH or IH and true δ_{CP} is $\pm 90°$ we get 4 possible combinations. From these figures one can read off the range of θ_{23} for which octant can be determined for $\delta_{CP} = \pm 90°$ at a specified C.L. We see for all the four cases of Fig. 5 that with $7 + 3$ years of $(\nu + \bar{\nu})$ run octant can be determined at 3σ (4σ) for $\delta_{CP} = \pm 90°$ excepting for the range $41.5° < \theta_{23} < 49°$ $(40.5° < \theta_{23} < 50.7°)$. From the figures we also see that $7 + 3$ and $5 + 5$ combinations give almost same sensitivity. However for the pure neutrino run the ranges are different

Table IV
Ranges of θ_{23} for which octant can be resolved at 3σ (4σ) for $[10+0]$ configuration for 10 kt detector.

True parameter	θ_{23} range for $3\sigma(4\sigma)$
NH, $\delta_{CP}=-90°$	$<39°(37.4°)$ and $>49°(50.6°)$
NH, $\delta_{CP}=90°$	$<43°(35.7)$ and $>53°(54°)$
IH, $\delta_{CP}=-90°$	$<37°(35.7)$ and $>49°(55°)$
IH, $\delta_{CP}=90°$	$<42°(40)$ and $>54°(55°)$

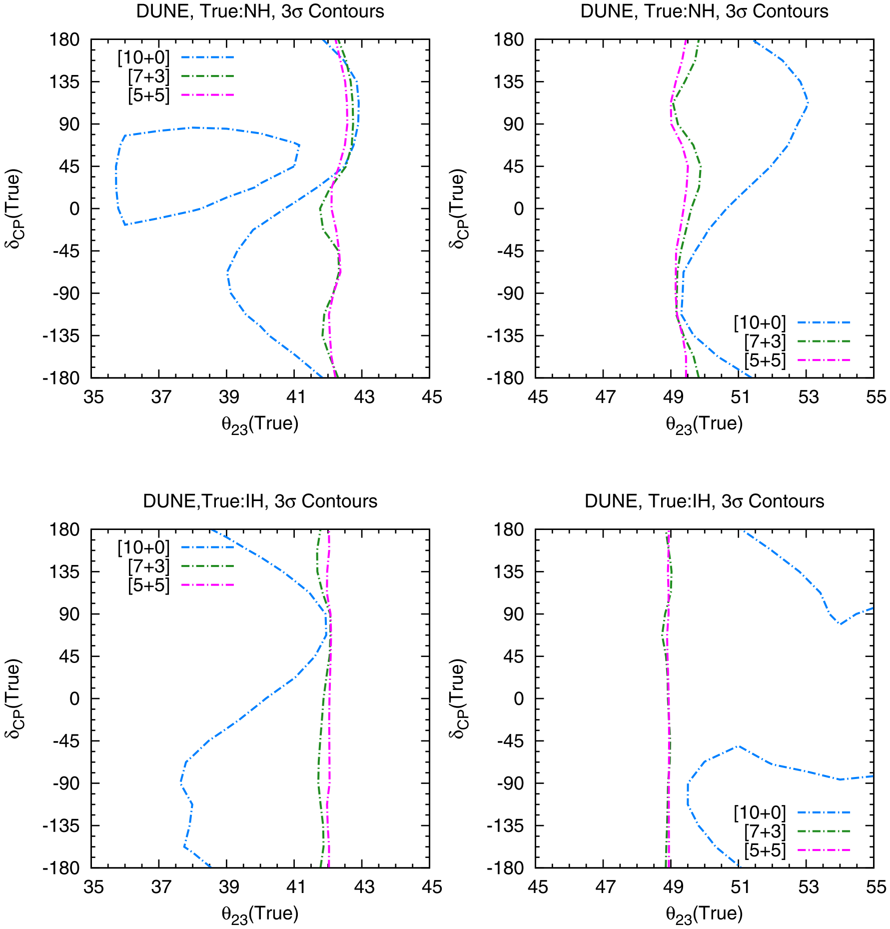

Fig. 6. Contour plots in true(θ_{23}, δ_{CP}) plane, here true hierarchy is NH (IH) for upper (lower) row and left (right) panel is for LO (HO). Marginalization over hierarchy is done. The allowed regions are to the right (left) side of the contours in the left (right) panel. (For interpretation of the references to color in this figure, the reader is referred to the web version of this article.)

and also vary depending on the true values of δ_{CP} and hierarchy. In Table IV we give the ranges of θ_{23} for which octant can be resolved at 3σ and 4σ with pure neutrino run.

So far we have focused on the cases for which either true θ_{23} was fixed or true δ_{CP} was fixed. In Fig. 6 we give the 3σ exclusion plots in true(θ_{23}–δ_{CP}) plane. We consider all possible true values of δ_{CP} from ($-180°$ to $+180°$) and θ_{23} in lower octant from 35°–45° and higher octant from 45°–55°. This figure shows the role of antineutrino run in the full range of allowed δ_{CP} and θ_{23} parameter space. The allowed region for the left (right) panel is the R.H.S. (L.H.S.) of each curve of the true(θ_{23}–δ_{CP}) plane.[2] We observe by comparing the left and the right panels that DUNE can provide better constraints on θ_{23} parameter space in case of LO as compared to HO. For NH-LO the antineutrino run is necessary for the LHP and part of UHP. Only in the range $90° < \delta_{CP} < 135°$ the only neutrino run i.e., the $[10 + 0]$ configuration gives a slightly better sensitivity. On the other hand for NH-HO the antineutrinos play a more prominent role for δ_{CP} in the UHP. For IH-LO the antineutrino run is again important apart from near $\delta_{CP} \sim 90°$, for which the improvement in sensitivity by adding antineutrinos is not very significant. For IH-HO the antineutrinos play important role in the full parameter space. Also the exclusion plots show that if true θ_{23} lies between (43°–49°) then it is not possible to resolve octant degeneracy at 3σ C.L. by DUNE using 10 kt detector. Overall one can say that antineutrino runs are necessary for most of the parameter region and $7 + 3$ and $5 + 5$ give similar sensitivities. Note that in the context of LBNO 75%–25% ($\nu - \bar{\nu}$) was recommended in [55].

Finally in Fig. 7 we plot the 3σ precision contours in the true θ_{23}–test θ_{23} plane for $\delta_{CP} = \pm 90°$. These figures reflect the relation between octant degeneracy and precision of θ_{23}. The upper panels are for normal hierarchy and the lower panels are for inverted hierarchy. From these plots we see that for pure neutrino run there are other allowed values of θ_{23} apart from the true value, if $\theta_{23} \in$ LO (HO) at $\delta_{CP} = -90°(+90°)$. This happens because of the octant degeneracy. As we have already seen, for $\delta_{CP} = -90°(+90°)$, neutrinos suffer from octant degeneracy in LO (HO) in both the hierarchies and this in turn affects the precision of θ_{23} which is clearly seen from the figures. Adding antineutrinos help to improve the precision and both $7 + 3$ and $5 + 5$ give almost similar precision of θ_{23}. But as one approaches the maximal value of θ_{23}, the precision becomes worse due to the difficulty in determining the octant around those values of θ_{23}.

4.2. Antineutrinos, octant degeneracy and CP discovery potential of DUNE

In this section we present the CP discovery χ^2 of DUNE as a function of true δ_{CP}. CP violation discovery potential of an experiment is defined by its capability of distinguishing a true value of δ_{CP} other than 0° and 180°. We present these figures for the case where hierarchy and octant are assumed to be unknown and known. The main aim of this section is to elucidate the role of antineutrinos in discovering δ_{CP} and the interconnection with the octant degeneracy.

The Fig. 8 plots the CP discovery χ^2 as function of true δ_{CP} for the case when hierarchy and octant are assumed to be unknown. From the different panels it is seen that:

- The antineutrino runs play an important role for (i) LO near true $\delta_{CP} = -90°$ and (ii) HO near true $\delta_{CP} = +90°$. This is true for both NH and IH. Note from Table II that these are the regions where neutrino probabilities exhibit octant degeneracy. Since antineutrino probabilities do not possess this degeneracy, addition of these helps in the removal of the degeneracy and enhancement of CP sensitivity.
- For true hierarchy as NH, $+90°$-LO and $-90°$-HO do not have octant degeneracy for neutrinos whereas antineutrinos have degeneracy (see Table II). Even then $7 + 3$ gives almost

[2] For NH-LO, DUNE$[10 + 0]$ (top left panel of Fig. 6), the area enclosed by the blue curve also corresponds to the allowed region.

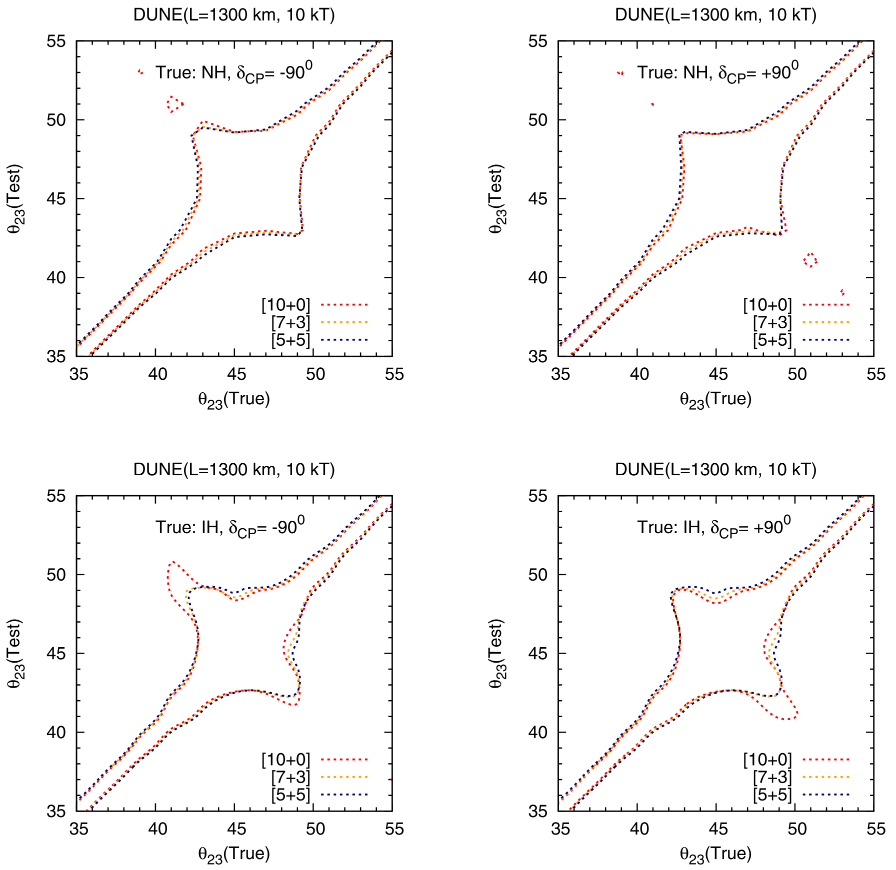

Fig. 7. θ_{23} precision plots of DUNE in True(θ_{23})–Test(θ_{23}) plane at 3σ C.L. Here top (bottom) row is for NH(IH).

same result as $10+0$ notwithstanding the loss of statistics. In both cases this happens due to tension between the neutrino and antineutrino χ^2s.

– For $+90°$-LO the minima for $10+0$ comes at $\delta_{CP} = 180°$ whereas replacing 3 years of neutrino run by antineutrino run shifts the χ^2_{min} at $\delta_{CP} = 0°$ where the neutrino contribution is higher and thus $7+3$ becomes comparable to $10+0$.

– For the case of $-90°$-HO and neutrinos the CPV χ^2 is a falling function of θ_{13}, and the minima comes at 0.109 while for $7+3$ it comes at 0.106. The neutrino contribution at $\sin^2\theta_{13} = 0.106$ being higher the overall χ^2 for $7+3$ becomes greater.

- Similarly, for true hierarchy IH, $+90°$-LO and $-90°$-HO are free from octant degeneracy for neutrinos. But still the CP sensitivity for these cases are slightly better for combined neutrino–antineutrino run (for both $7+3$ and $5+5$ case) as compared to pure neutrino run. This happens because due to matter effects the $P_{\bar{\mu}\bar{e}}$ is higher than $P_{\mu e}$ for IH (see Fig. 1). Thus addition of antineutrinos enhances the appearance χ^2.

In Fig. 9 we present the same plots as that of Fig. 8 but assuming the hierarchy and octant to be known.

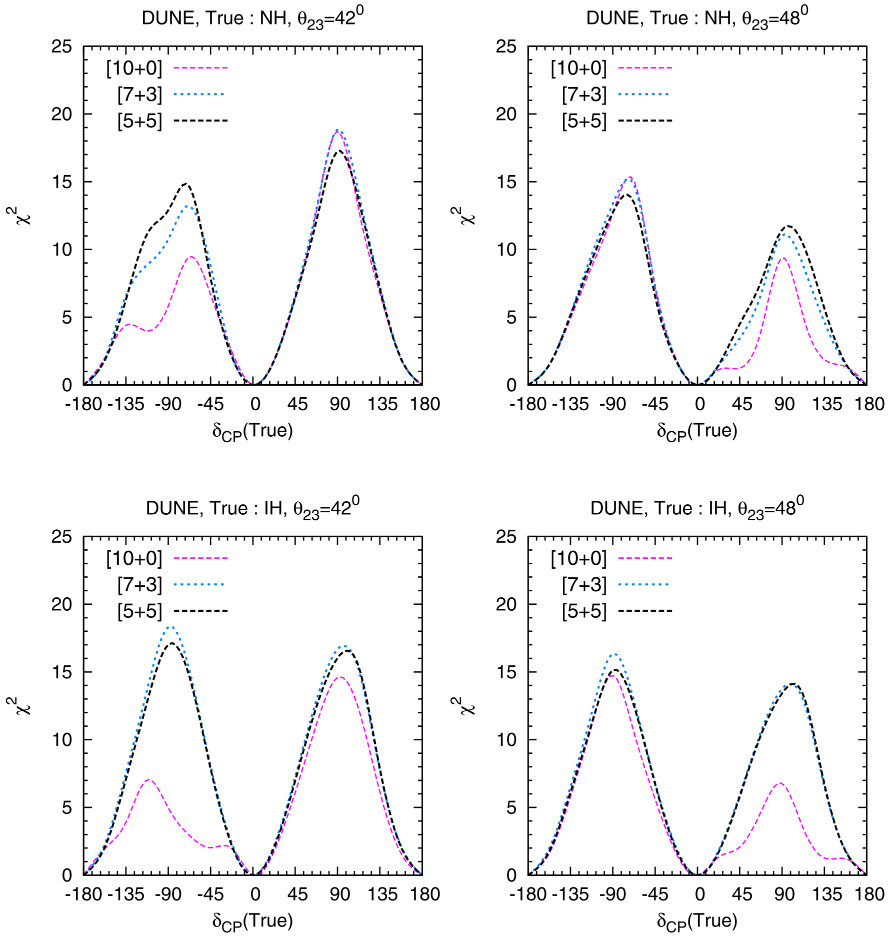

Fig. 8. CPV χ^2 for DUNE when hierarchy and octant are unknown.

- Comparing with the plots in Fig. 8 we see that the CP sensitivity for $-90°$-LO improves for the $10+0$ case, for both the hierarchies. In fact for $-90°$-LO-NH, $10+0$ gives the best sensitivity if the octant is known. This establishes the fact that, the antineutrino run was instrumental for removing the wrong octant solutions.
- For $+90°$-NH-HO although there is some improvement for the $10+0$ case as compared to the case of unknown octant, the CP sensitivity of $7+3$ and $5+5$ are still better than $10+0$. This implies that though octant is known, antineutrinos play some role in enhancing the CP sensitivity.
  - To understand the above point in more detail in Fig. 10 we plot the CPV discovery χ^2 for different channels vs test θ_{23} in the correct octant (since octant is assumed to be known) for a particular value of true δ_{CP}. The top left panel of Fig. 10 shows that, for neutrinos and true value of $+90°$-NH-$48°$, the CP sensitivity of the appearance channel is an increasing function of test θ_{23}. But as the precision of θ_{23} (which comes from the disappearance channel) is poor near the maximal value, the combined χ^2 minimum does not occur at the true θ_{23} value (which is $\theta_{23} = 48°$) but occurs at $\theta_{23} = 45°$. For antineutrinos (top right

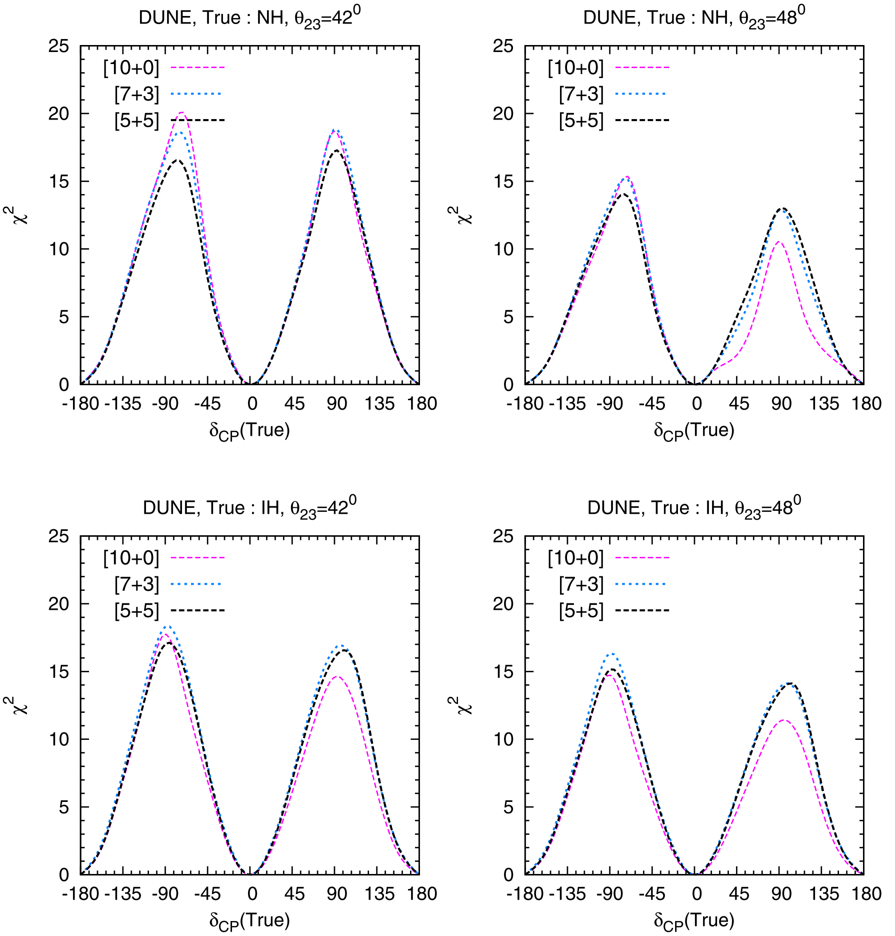

Fig. 9. CPV χ^2 for DUNE when hierarchy and octant are known.

panel), the nature of the disappearance channel χ^2 is same as that of neutrinos but the appearance χ^2 decreases as test θ_{23} increases. Because of this opposite behaviour when antineutrinos are combined with neutrinos, the χ^2 minima shifts to the correct value of θ_{23} and the overall CP sensitivity at the true point is enhanced. The poor θ_{23} precision of $+90°$-HO-NH in neutrinos arise due to the higher matter effect. Due to which the subleading matter terms start to contribute in the disappearance channel which affect the θ_{23} precision. Note that this does not happen for $-90°$-NH-HO (despite matter is high) because even though the precision of θ_{23} is poor near the maximal value of θ_{23} for $\delta_{CP} = -90°$ the appearance channel sensitivity is a decreasing function of test θ_{23} and this causes the overall minima to occur at the correct value of θ_{23}. This can be seen from the right panel of the middle row of Fig. 10.

– Also note that for true $+90°$-NH $42°$ (left panel of middle row of Fig. 10), the precision of θ_{23} near the maximal value is quite good as compared to $\theta_{23} = 48°$. This is because for lower octant, the denominator in the χ^2 is smaller as compared to that in HO and thus a better θ_{23} precision is obtained.

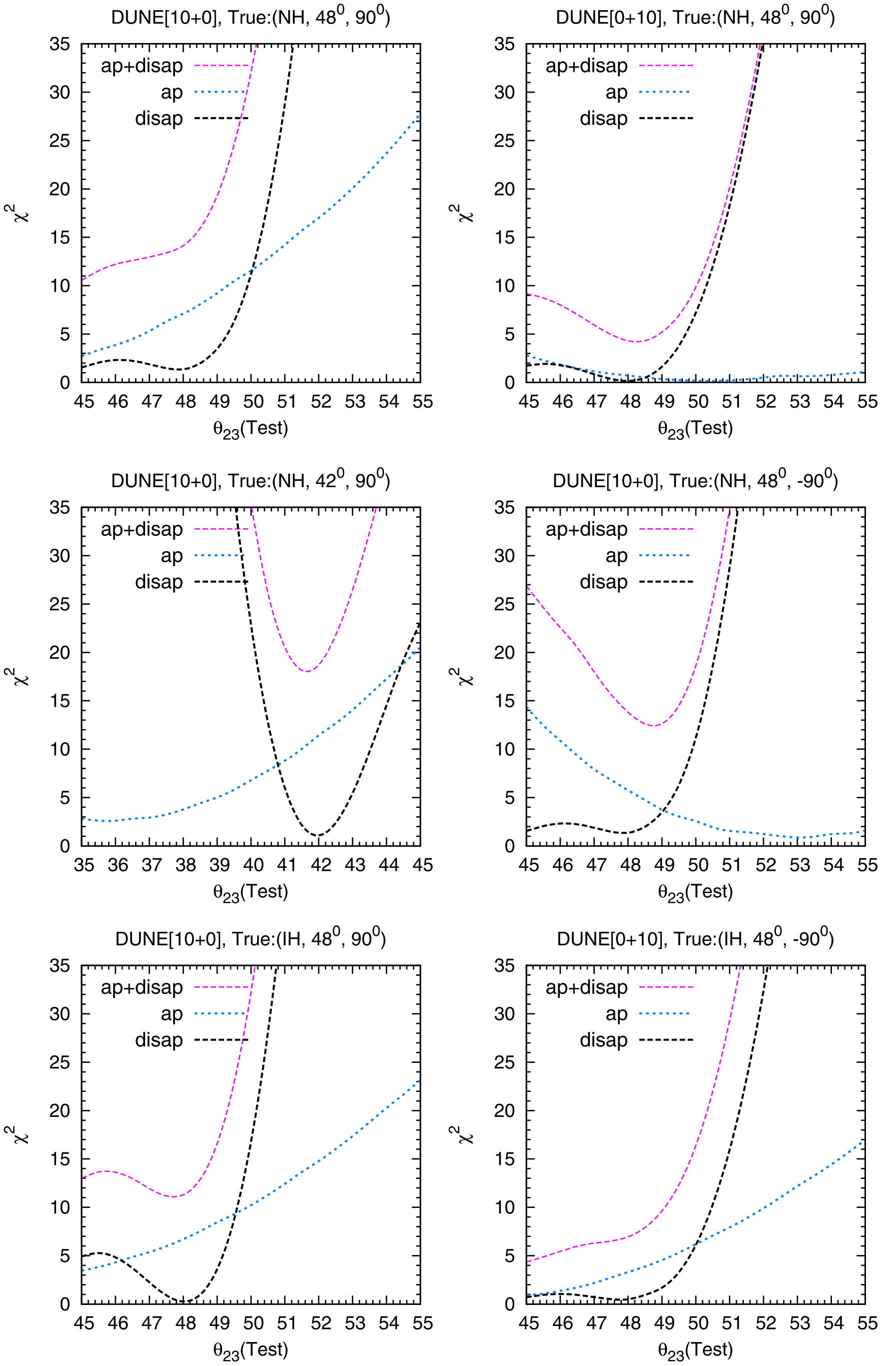

Fig. 10. CPV χ^2 for DUNE when hierarchy and octant are known.

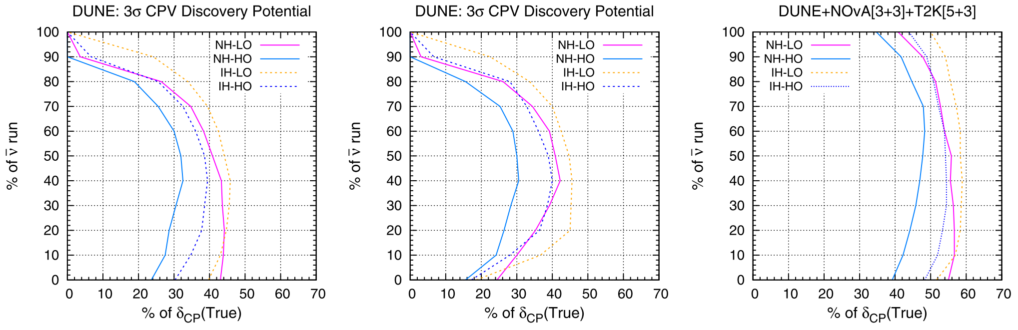

Fig. 11. CP violation discovery χ^2 at 3σ C.L. in (% of $\delta_{CP}(True)$, % of antineutrino run) plane. Here, first and second column are for DUNE and third column is for DUNE + NOνA[3 + 3] + T2K[5 + 3]. Also y-axis represents the % of antineutrino run out of total 10 years of $[\nu + \bar{\nu}]$ run in DUNE. In first (second and third) column we consider hierarchy and octant are known (unknown).

   – For true hierarchy IH, even $\theta_{23} = 48°$ has a good precision near the maximal value for neutrinos (bottom left panel of Fig. 10). This is because for IH the matter effect is less for neutrinos and thus θ_{23} precision measurement capability of the disappearance channel is better as can be seen comparing the top and bottom left panels of Fig. 10. But since the matter effect is more for antineutrinos, the precision of θ_{23} for IH and antineutrinos is poor (bottom right panel).

- Similarly for $+90°$-HO-IH although the octant is known the antineutrino run gives an enhanced χ^2. This is due to matter effects in antineutrinos for IH which makes $P_{\bar{\mu}\bar{e}}$ higher than the corresponding neutrino probabilities (see Fig. 1). This increases the appearance χ^2 in presence of antineutrinos. For similar reasons the χ^2 for $7+3$ is slightly higher than $10+0$ for $-90°$-LO-IH.

In the first and second panels of Fig. 11, we plot the percentage of antineutrino run vs percentage of δ_{CP} values for which CP violated can be discovered at 3σ C.L. in DUNE for four cases encompassing both hierarchies and octants. The first (second) panel represents when octant and hierarchy are known (unknown). From both plots it is seen that with dominant antineutrino or neutrino run a lesser CP fraction is reached. Overall 40% antineutrino run seems to be optimum in all cases. Comparing these two plots it is seen that when octant is known then greater percentage of CP fraction can be probed with less antineutrino component. The maximum CP coverage can be achieved for IH-HO and minimum for NH-HO.

In the third panel of Fig. 11 the same is plotted by combining NOνA and T2K with DUNE. From the figure we can see that the percentage of δ_{CP} that can be probed is enhanced in all cases. The curves are now much flatter implying that even with pure neutrino or antineutrino runs considerable CP coverage can be obtained. This is due to the contribution from NOνA and T2K. In Fig. 12 we show the dependence of percentage of δ_{CP} that can be probed as a function θ_{23}. This figure is drawn assuming 60% neutrino and 40% antineutrino run which is the optimal configuration as seen in Fig. 11. The coverage of δ_{CP} for which CP violation can be discovered at 3σ C.L. is better for IH. For NH specially close to 45° the coverage is less due to the poor precision of θ_{23} as discussed earlier.

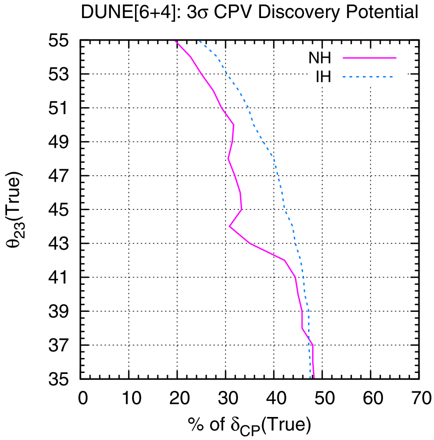

Fig. 12. CP violation discovery χ^2 at 3σ C.L. for DUNE[6 + 4] for all true θ_{23} when hierarchy and octant are unknown.

5. Summary and conclusions

In this paper we perform a detailed investigation of the octant and δ_{CP} sensitivity of the future generation superbeam experiment DUNE which has a baseline of 1300 km. We analyze in detail the physics of the antineutrinos for the DUNE baseline and what kind of synergy can be offered by the addition of antineutrinos to pure neutrino runs. In the context of the long baseline experiments with source–detector distance <1000 km it is well known that the octant sensitivity comes mainly from the combination of $P_{\mu e}$ and $P_{\mu\mu}$ channels. For $P_{\mu e}$ channel the χ^2 is a rising function of θ_{23} and consequently the minima in the wrong octant always comes at 45°. On the other hand $P_{\mu\mu}$ being governed by $\sin^2 2\theta_{23}$, the minima comes close to $\pi/2 - \theta_{23}$ with no octant sensitivity. When both channels are combined then the global minima comes closer to $\pi/2 - \theta_{23}$ where the appearance channel contributes a large octant sensitive χ^2. However the appearance channel is also affected by the occurrence of octant–δ_{CP} degeneracy which can lead to spurious solutions. The nature of this degeneracy is the same for both the hierarchies but has a complementary nature for neutrinos and antineutrinos i.e., the δ_{CP} and octant combination for which there is degeneracy in neutrinos is devoid of this for antineutrinos. The upshot is that the combination of neutrino and antineutrino runs helps to solve this degeneracy. On the other hand the statistics is more for neutrinos. This leads to the question of what is the optimal combination of neutrino and antineutrino run for giving the maximum benefit for octant determination. This issue has been addressed in this work in the context of the DUNE experiment. We also discuss to what extent the broad-band nature of the beam and enhanced matter effect influences the octant sensitivity and if any new features emerge as compared to the previous narrow-band off-axis experiments with baseline <1000 km. We find that for the DUNE baseline addition of antineutrinos are helpful in general. This statement holds true even when there may be some degeneracy associated with the antineutrino channel and one expects the pure neutrino run to give the best results. This occurs because of opposing tendencies of neutrino and antineutrino χ^2s. We find that when $\bar{\nu}$ is combined with ν then the overall χ^2 minimum is still governed by the neutrinos because of higher statistics. At this point the antineutrino contribution to χ^2 is higher and hence adding these enhances octant sensitivity inspite of the associated octant degeneracy. One should also note that due to the broadband nature of the beam the degeneracy may be limited for few energy bins only. Note that, due to the broad-band nature of the beam, the octant sensitivity coming from pure neutrino run is also quite high at the true values where neutrino probabilities are themselves degenerate. The antineutrino contribution can be more for IH since due to enhanced matter effects the corresponding probabilities can be much higher than the neutrino probabilities. Thus even if the main octant sensitivity comes from the neutrinos, the broad-band nature compounded with the higher matter effect leads to some octant sensitivity coming from antineutrino channels in case of IH. In addition we find that a small octant sensitive contribution comes from the disappearance channel when neutrino and antineutrino runs are combined although pure neutrino or pure antineutrino runs do not have this sensitivity. This happens because, due to matter effect the neutrino and antineutrino probabilities are slightly different and hence the minima comes at slightly different position for each case. When combined, there is a tension between these two which gives rise to a small octant sensitive χ^2 contribution. Note that these features arising due to matter effects have not been highlighted in the literature earlier.

Taking two representative values of θ_{23} in the lower octant (39°) and higher octant (51°) we study the behaviour of χ^2 with δ_{CP} for both NH and IH. We find that for a 10 kt mass of the detector although for some δ_{CP} values (3–4)σ sensitivity can be achieved with only neutrino run, overall adding antineutrinos is helpful. For a $7+3$ year $(\nu+\bar{\nu})$ run, close to 4σ sensitivity can be achieved over all values of δ_{CP}. It is found that $7+3$ and $5+5$ do not give significantly different results. We compute the χ^2 as a function of true θ_{23} for maximum CP violation. From this study we find that with $7+3$ years option octant degeneracy can be resolved at 3σ excepting the range $41.5° < \theta_{23} < 49°$. Increasing the antineutrino component and making runtime $5+5$ does not make any discernible difference to the results. Finally we also study the octant sensitivity in the true(θ_{23}–δ_{CP}) plane which checks the validity of the conclusions drawn earlier over the whole parameter range. We find that for 10 kt year mass the antineutrino run enhances the range of θ_{23} over which octant sensitivity can be achieved. Including antineutrino runs, octant sensitivity can be obtained at 3σ excepting the range $43° < \theta_{23} < 49°$ not only for maximal violation of δ_{CP} but over the whole range. In this case with only neutrino run octant remains undetermined over a large parameter space. We also present the 3σ precision contours in the true θ_{23}–test θ_{23} plane. These plots show that adding antineutrino runs also help in obtaining improved precision on θ_{23}.

We also present results on the CP violation discovery potential of DUNE emphasizing the role played by the antineutrinos. The CP sensitivity of any long-baseline experiment is affected by the occurrence of the wrong-hierarchy–wrong octant–wrong δ_{CP} solutions. Since the antineutrinos help in removing these solutions, one of the main role of the antineutrinos in enhancing CP sensitivity is to remove these wrong solutions. We present results for cases where hierarchy and octant are unknown and known and compare the role of the antineutrinos in both situations. We find that when octant is not known then in parameter spaces where octant degeneracy is manifest the antineutrino component increases CP sensitivity by removing wrong octant solutions. This is the case for instance for LO, $\delta_{CP} \sim -90°$ and HO, $\delta_{CP} \sim +90°$ for both hierarchies. However even when the octant is known addition of antineutrinos can improve the result because of the tension between the two χ^2s which raises the overall χ^2. The contribution from the antineutrino channel is higher for IH since due to matter effects the antineutrino probability is higher than the corresponding neutrino probability. At $\delta_{CP} = \pm 90°$, a greater than 3σ sensitivity is achieved in all cases. We have also explored how addition of antineutrinos affects the fraction of δ_{CP} values for which CP sensitivity can be probed at 3σ level. We find that when octant is known, same sensitivity can be achieved with a lesser fraction of antineutrinos for both hierarchies. The maximum CP fraction is achieved for IH-LO. Overall the best result comes with 60% neutrino and 40% antineutrino runs for all the four cases.

In conclusion, we have explored the role of antineutrinos in enhancing octant and CP sensitivity for a 1300 km experiment with a broad-band beam as is planned by the DUNE collaboration. We emphasize on the importance of antineutrino run in resolving octant ambiguity and increasing CP sensitivity. Although for some specific parameters only neutrino run can give 3σ octant sensitivity for a 10 kt detector mass of DUNE, overall a balanced neutrino–antineutrino run gives better sensitivity. For the case of δ_{CP} discovery also in most of the parameter space antineutrinos play an important role due to synergistic effects between neutrinos and antineutrinos even under the assumption of octant to be known.

Acknowledgements

The authors would like to thank Sushant K. Raut for his help in GLoBES and also for many useful discussions regarding DUNE.

References

[1] K. Eguchi, et al., KamLAND, Phys. Rev. Lett. 92 (2004) 071301, arXiv:hep-ex/0310047.
[2] R. Wendell, et al., Super-Kamiokande Collaboration, Phys. Rev. D 81 (2010) 092004, arXiv:1002.3471.
[3] P. Adamson, et al., MINOS Collaboration, Phys. Rev. Lett. 112 (2014) 191801, arXiv:1403.0867.
[4] K. Abe, et al., T2K Collaboration, arXiv:1409.7469, 2014.
[5] M.C. Gonzalez-Garcia, M. Maltoni, T. Schwetz, Nucl. Phys. B 908 (2016) 199, arXiv:1512.06856.
[6] F. Capozzi, E. Lisi, A. Marrone, D. Montanino, A. Palazzo, Nucl. Phys. B 908 (2016) 218, arXiv:1601.07777.
[7] K. Abe, et al., T2K, Phys. Rev. D 91 (2015) 072010, arXiv:1502.01550.
[8] P. Adamson, et al., NOvA, Phys. Rev. Lett. 116 (2016) 151806, arXiv:1601.05022.
[9] P. Adamson, et al., NOvA, Phys. Rev. D 93 (2016) 051104, arXiv:1601.05037.
[10] V. Barger, D. Marfatia, K. Whisnant, Phys. Rev. D 65 (2002) 073023, arXiv:hep-ph/0112119.
[11] J. Burguet-Castell, M. Gavela, J. Gomez-Cadenas, P. Hernandez, O. Mena, Nucl. Phys. B 646 (2002) 301, arXiv:hep-ph/0207080.
[12] H. Minakata, H. Nunokawa, J. High Energy Phys. 0110 (2001) 001, arXiv:hep-ph/0108085.
[13] G.L. Fogli, E. Lisi, Phys. Rev. D 54 (1996) 3667, arXiv:hep-ph/9604415.
[14] K. Abe, et al., T2K, Phys. Rev. Lett. 107 (2011) 041801, arXiv:1106.2822.
[15] Y. Abe, et al., Double Chooz Collaboration, J. High Energy Phys. 1410 (2014) 86, arXiv:1406.7763.
[16] F.P. An, et al., Phys. Rev. Lett. 115 (2015) 111802, arXiv:1505.03456.
[17] J. Ahn, et al., RENO Collaboration, Phys. Rev. Lett. 108 (2012) 191802, arXiv:1204.0626.
[18] S. Prakash, S.K. Raut, S.U. Sankar, Phys. Rev. D 86 (2012) 033012, arXiv:1201.6485.
[19] S.K. Agarwalla, S. Prakash, S.U. Sankar, J. High Energy Phys. 1307 (2013) 131, arXiv:1301.2574.
[20] P. Machado, H. Minakata, H. Nunokawa, R.Z. Funchal, arXiv:1307.3248, 2013.
[21] P. Coloma, H. Minakata, S.J. Parke, Phys. Rev. D 90 (2014) 093003, arXiv:1406.2551.
[22] M. Ghosh, P. Ghoshal, S. Goswami, N. Nath, S.K. Raut, Phys. Rev. D 93 (2016) 013013, arXiv:1504.06283.
[23] P. Huber, M. Lindner, T. Schwetz, W. Winter, J. High Energy Phys. 11 (2009) 044, arXiv:0907.1896.
[24] H. Minakata, H. Sugiyama, Phys. Lett. B 580 (2004) 216, arXiv:hep-ph/0309323.
[25] A. Chatterjee, P. Ghoshal, S. Goswami, S.K. Raut, J. High Energy Phys. 1306 (2013) 010, arXiv:1302.1370.
[26] J. Kameda, Talk given at NuFact, 2015.
[27] S. Choubey, P. Roy, Phys. Rev. Lett. 93 (2004) 021803, arXiv:hep-ph/0310316.
[28] O.L.G. Peres, A.Y. Smirnov, Phys. Lett. B 456 (1999) 204, arXiv:hep-ph/9902312.
[29] M.C. Gonzalez-Garcia, M. Maltoni, A.Yu. Smirnov, Phys. Rev. D 70 (2004) 093005, arXiv:hep-ph/0408170.
[30] S. Choubey, A. Ghosh, J. High Energy Phys. 1311 (2013) 166, arXiv:1309.5760.
[31] M. Ghosh, P. Ghoshal, S. Goswami, S.K. Raut, Nucl. Phys. B 884 (2014) 274, arXiv:1401.7243.
[32] M. Ghosh, Phys. Rev. D 93 (2016) 073003, arXiv:1512.02226.
[33] J. Evslin, S.-F. Ge, K. Hagiwara, J. High Energy Phys. 02 (2016) 137, arXiv:1506.05023.
[34] C. Adams, et al., LBNE Collaboration, arXiv:1307.7335, 2013.
[35] S.K. Agarwalla, S. Prakash, S. Uma Sankar, J. High Energy Phys. 1403 (2014) 087, arXiv:1304.3251.
[36] M. Ghosh, S. Goswami, S.K. Raut, ArXiv e-prints, arXiv:1412.1744, 2014.

[37] K. Bora, D. Dutta, P. Ghoshal, Mod. Phys. Lett. A 30 (2015) 1550066, arXiv:1405.7482.

[38] V. Barger, A. Bhattacharya, A. Chatterjee, R. Gandhi, D. Marfatia, et al., Phys. Rev. D 89 (2014) 011302, arXiv:1307.2519.

[39] V. Barger, A. Bhattacharya, A. Chatterjee, R. Gandhi, D. Marfatia, et al., arXiv:1405.1054, 2014.

[40] K.N. Deepthi, C. Soumya, R. Mohanta, New J. Phys. 17 (2015) 023035, arXiv:1409.2343.

[41] S.K. Agarwalla, T. Li, A. Rubbia, J. High Energy Phys. 1205 (2012) 154, arXiv:1109.6526.

[42] P. Huber, M. Lindner, W. Winter, Comput. Phys. Commun. 167 (2005) 195, arXiv:hep-ph/0407333.

[43] P. Huber, J. Kopp, M. Lindner, M. Rolinec, W. Winter, Comput. Phys. Commun. 177 (2007) 432, arXiv:hep-ph/0701187.

[44] R. Acciarri, et al., DUNE, arXiv:1512.06148, 2015.

[45] D. Cherdack, Private communication, 2014.

[46] M.C. Gonzalez-Garcia, M. Maltoni, T. Schwetz, J. High Energy Phys. 11 (2014) 052, arXiv:1409.5439.

[47] F. Capozzi, G. Fogli, E. Lisi, A. Marrone, D. Montanino, et al., Phys. Rev. D 89 (2014) 093018, arXiv:1312.2878.

[48] D. Forero, M. Tortola, J. Valle, arXiv:1405.7540, 2014.

[49] M.C. Gonzalez-Garcia, M. Maltoni, Phys. Rev. D 70 (2004) 033010, arXiv:hep-ph/0404085.

[50] G. Fogli, E. Lisi, A. Marrone, D. Montanino, A. Palazzo, Phys. Rev. D 66 (2002) 053010, arXiv:hep-ph/0206162.

[51] R. Gandhi, et al., Phys. Rev. D 76 (2007) 073012, arXiv:0707.1723.

[52] E.K. Akhmedov, R. Johansson, M. Lindner, T. Ohlsson, T. Schwetz, J. High Energy Phys. 04 (2004) 078, arXiv:hep-ph/0402175.

[53] A. Cervera, et al., Nucl. Phys. B 579 (2000) 17, arXiv:hep-ph/0002108.

[54] M. Freund, Phys. Rev. D 64 (2001) 053003, arXiv:hep-ph/0103300.

[55] C.R. Das, J. Maalampi, J. Pulido, S. Vihonen, J. High Energy Phys. 02 (2015) 048, arXiv:1411.2829.